The 2010 IEEE/RSJ International Conference on
Intelligent Robots and Systems
October 18-22, 2010, Taipei, Taiwan

Energy Management for Four-Wheel Independent Driving Vehicle

Huihuan Qian, Guoqing Xu, Jingyu Yan, Tin Lun Lam, Yangsheng Xu, and Kun Xu

Abstract— **The promising electric vehicle (EV) technology is a direction to tackle the global non-renewable energy problem. However, the efficiency to use the electric energy still needs deliberate research. Traditional EV has no choice to manage its energy flow, because it has only one traction motor. With the robotic research in 4 wheel independent drive (4WID), the driving task of the single traction motor can be shared by 4 independent in-wheel motors. By exploring the motor efficiency map, we propose the energy management strategy based on optimal driving torque distribution(ODTD). The total input power of the 4 motors can be minimized while the driving performance is still maintained, and electric energy consumption can be reduced compared with traditional single motor driving EV. Simulation results validate the proposed strategy. The energy management strategy can also be applied to multi-driving-wheel mobile robots.**

I. INTRODUCTION

Energy has been a global problem facing the overall human world and societies. The non-renewable energy source, especially oil, on which we are tightly dependent nowadays, will ultimately reach the end, if no solution is made to its massive usage. Within all the fuel consumption fields, transportation has accounted for a significantly large portion. Encouragingly, lots of efforts have been made to enhance the energy usage efficiency and reduce the energy loss. They include both technological solutions and non-tech solutions[4]. There have been also a large amount of explorations for new energy sources, for instances, electric batteries, fuel cells, flywheels and so on. Electric energy flows in the powertrain for final propelling the vehicle by motor(s).

In the vehicle research, hybrid electric vehicles (HEVs) and EVs are developed and improved with the goal to transform electric energy to kinematic energy with high efficiency. Much endeavor has been devoted to the area how to manage the energies from the engine and the motor in HEVs[15][16][17][18]. There are commercialized HEVs, such as Toyota Prius[19], Honda Civic HEV[20], and BYD Dual Mode F3[21], etc. Energy management in EVs probes the reduction of energy expenditure by auxiliary devices such as air conditioner and lighting when the surrounding permits[1], wheel slippage reduction[8], and dual energy sources of battery and ultra capacitor[2][3].

In the robotic field, 4 wheel independent drive (4WID) or direct drive technologies have resulted in a rich literature in mobile robots. Some examples are Titan[23], a 4WD wheelchair[24], a 4-Wheel Differentially Steered (4WDS) mobile robot[25], a 4-wheel Omni-directional Mobile Robot[26], and so on. Within these research, traction control and robot traversability have attracted the much attention[9][6]. Few research in robotic area is focused on the energy management in the 4WID configuration. This might be due to the non-urgency of the energy saving issue in the relatively small quantity of robots.

Recently, the 4WID/direct drive concept has been introduced into the vehicle field and make a vehicle more like a robot. Nissan Pivo2 has 4 in-wheel motors[22]; COMS3-A[5] and QUNO[11] both have two in-wheel motors in the rear; [10] proposed a structure with 4 in-wheel motors; Omni-directional Kart-1[27] integrates 4 in-wheel motor and 4 steering motor, and it can have omni-directional motions.

The 4WID configuration has the potential for attempt to further reduce energy consumption. In a traditional EV, one large-power traction motor is responsible for propelling the whole vehicle[12]. In an established driving cycle, there is no degree of freedom for this traction motor to select operation points in its high efficiency region. Nevertheless, if the number of motors increases to $\mathrm{N}(\mathrm{N} > 1)$, several small powered motors can work together, and the DOF is increased to $\mathrm{N} - 1$. Thus, energy management strategy can be optimized to choose the operation points of each motor, so as to further improve the energy usage efficiency. Such the robotic 4WID structure enables us to further reduce the electric energy consumption by coordinating the different motors.

The motor used in transportation equipment in the late 1990s reaches approximately 1800 TWh/year in US[13]. With the gradual introduction of EV into the market, this number will be significantly increase. Thus, the potential energy saving can also share a big portion if appropriate energy management strategy is developed.

This paper is organized as follows. In Section II, vehicle dynamic model, motor model, as well as battery and gearbox models are introduced. Section III discusses on the optimization conditions based on the motor model and explores the motor operation region in which it is sufficient to find energy management strategy based on optimal driving torque distribution (ODTD). Energy management strategy and system flow chart are elaborated in Section IV. In Section V, simulation results are illustrated to validate the strategy. Section VI concludes the paper.

II. MODELING

A. Vehicle Dynamic Model

The 4WID configuration is illustrated in Fig. 1.

H. Qian, G. Xu, J. Yan, T. L. Lam, and Y. Xu are with the Shenzhen Institutes of Advanced Technology, Chinese Academy of Sciences, Shenzhen, China, and the Department of Mechanical and Automation Engineering, The Chinese University of Hong Kong, Hong Kong SAR, China. {hhqian, gqxu, jyyan, tllam, ysxu}@mae.cuhk.edu.hk

K. Xu is with the Shenzhen Institutes of Advanced Technology, Chinese Academy of Sciences, Shenzhen, China. kun.xu@siat.ac.cn

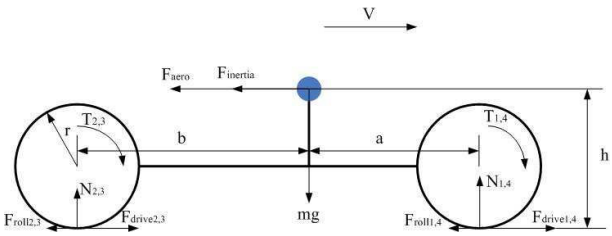

Fig. 1. 4WID configuration

TABLE I
DENOTATION

Parameter	Symbol	Unit	Value
Vehicle total mass	m	kg	1144
Wheel radius	r	m	0.282
Wheel inertia	I_{wh}	kgm^2	3.2639
Center of gravity (CG) height	h	m	0.5
Distance (front axis to CG)	a	m	1.04
Distance (rear axis to CG)	b	m	1.56
Rolling resistance coefficient	μ_r		0.009
Maximal adhesive coefficient	μ		0.9
Air friction coefficient	C_D		0.335
Wind contact area	A	m^2	2
Air density	ρ	kg/m^3	1.2
Traditional EV gearbox ratio	ζ		6.6732

The elevation of the road is zero. N_i $(i = 1, 2, 3, 4)$ are the road upthrust force on the left-front, left-rear, right-rear and right-front wheels, respectively. F_{drivei} , F_{rolli}, and T_i $(i = 1, 2, 3, 4)$ are the driving force directly generated by tyre-road friction, rolling friction, and torque of the in-wheel motor, respectively, with the same indexing rule as the upthrust force. $F_{inertia}$ and F_{aero} are the dragging forces due to the vehicle inertia acceleration/deceleration and the aerodynamic friction, respectively. All other denotation and values are indicated in Table I. The vehicle parameters are based on the Smartcar EV configuration in Advisor.

The vehicle dynamic equations can be derived as below. They are utilized to compute the total driving torque T_{total} for each second in a driving cycle.

$$\sum_{i=1}^{4} F_{drivei} = F_{slope} + F_{aero} + F_{inertia} + \sum_{i=1}^{4} F_{rolli} \quad (1)$$

$$F_{slope} = mgcos(\theta) \quad (2)$$

$$F_{aero} = \frac{1}{2} C_D A \rho v^2 \quad (3)$$

$$F_{inertia} = m\frac{dv}{dt} \quad (4)$$

$$F_{rolli} = \mu_r N_i \quad (5)$$

$$N_{1,4} = \frac{1}{a+b}(mgbcos(\theta) - (F_{aero} + F_{inertia} + F_{slope})h) \quad (6)$$

$$N_{2,3} = \frac{1}{a+b}(mgacos(\theta) + (F_{aero} + F_{inertia} + F_{slope})h) \quad (7)$$

$$F_{drivei} \leq \mu N_i \quad (8)$$

$$T_i = r(F_{drivei} - F_{rolli}) + \frac{I_{wh}}{r}\frac{dv}{dt} \quad (9)$$

From (1) and (8), the total torque is

$$T_{total} = \sum_{i=1}^{4} T_i = r(F_{aero} + F_{inertia}) + \frac{4I_{wh}}{r}\frac{dv}{dt} \quad (10)$$

From (7), T_i should satisfy the constraint

$$T_i \leq r(\mu N_i - F_{rolli}) + \frac{I_{wh}}{r}\frac{dv}{dt} \quad (11)$$

B. Electric Motor Model

The Smartcar EV is propelled by a 75kW motor (MC_AC75) with peak efficiency 0.92. Motor efficiency map[7] is key to evaluate its performance. Fig. 2 visualizes the efficiency map, which we will concentrate on in the later sections for energy management. For a fair comparison, the 4WID vehicle utilizes the similar efficiency map with only speed and torque scaling factors α and β, and keep the total power equivalent to that of MC_AC75.

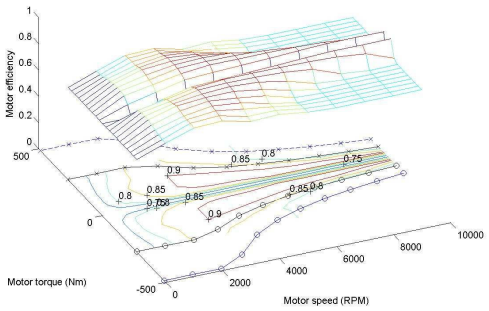

Fig. 2. Electric Motor Model

$$\eta_i(\omega_i, T_i) = \eta_0(\omega_{0i}, T_{0i}) \quad (12)$$

$$\omega_i = \alpha \times \omega_{0i} \quad (13)$$

$$T_i = \beta \times T_{0i} \quad (14)$$

where $\eta_i(\cdot,\cdot)$, ω_i and T_i $(i = 1, 2, 3, 4)$ are the efficiency, speed and torque of the left-front, left-rear, right-rear and right-front in-wheel motor, respectively; $\eta_0(\cdot,\cdot)$ is the efficiency map of the single traction motor; (ω_{0i}, T_{0i}) are the speed and torque mapped from (ω_i, T_i) by scaling factors α and β. $\alpha \times \beta = \frac{1}{4}$ to satisfy the total power constraint. The in-wheel motor speed scalar $\alpha = 0.1$, and the torque scalar $\beta = 2.5$. It should be noted that (ω_{0i}, T_{0i}) is not the operation point (ω_0, T_0) of the single traction motor in the same cycle point.

C. Battery Model

We adopt the internal resistance model to cope with the Smartcar EV model, because our emphasis is not on the battery management. State of charge (SOC) determine the open circuit voltage (V_{oc}) and the internal resistance of the battery. It is a lead-acid battery package consisting of 25 cells, with capacity of 25Ah and nominal voltage of 308V.

D. Gearbox Model

In the 4WID vehicle, because we utilize 4 independent in-wheel motors for direct propelling, there is no need for gearbox. However, in the traditional EV structure, gearbox is required to reduce the speed of motor output shaft and increase the torque for final wheel drive. The reduction ratio is 6.6732 based on the Smartcar EV model. We assume the efficiency of the transmission in the traditional EV to be 1, so as to see more clearly the energy saving effect by torque distribution. Normally, the transmission efficiency is about 0.9 in general operation points.

III. OPTIMIZATION CONDITIONS

A. Assumptions

1) In order to compare the performance of single-motor driving vehicle and the 4WID vehicle, the efficiency map of the motors are assumed to be similar as mentioned in Section II, i.e., the efficiency map of in-wheel motors are only transformed from the single traction motor by two scaling factors in speed domain and torque domain.

2) In order not to decrease the vehicle stability, the torques are distributed between the front and rear axis. Then the axle torque are distributed evenly between the left and right wheels. In that case, no yawing moment will be generated.

3) The efficiency of the transmission in the traditional EV to be 1. Hence, the traditional EV model performs better than normally.

4) The wheels are under non-slippery assumption.

B. Operation Region with Sufficient Condition for Optimal Torque Distribution

In this subsection, we will explore the operation region in the motor working space, in which the operation points have sufficient condition to guarantee energy saving strategy. We consider the motor propelling state. The regenerative state is neglected, because it will include braking torque distribution between frictional braking and regenerative braking, and if considered, it will distract our focus in the energy management by driving torque distribution.

In the single motor propelling EV,

$$\omega_0 = \omega_{wh}\zeta \tag{15}$$

$$T_0 = \frac{T_{total}}{\zeta \eta_{gb}} \tag{16}$$

Thus the total input power of the single motor is

$$P_0 = \frac{\omega_0 T_0}{\eta_0(\omega_0, T_0)} = \frac{\omega_{wh} T_{total}}{\eta_{gb}\eta_0(\omega_0, T_0)} \tag{17}$$

where ω_0 and T_0 output rotational speed and torque of the single traction motor, $\zeta = 6.6732$ is gearbox ratio, $\eta_{gb} = 1$ is the gearbox efficiency as assumed above.

In the 4WID vehicle,

$$\omega_{1,2,3,4} = \omega_{wh} \tag{18}$$

$$T_{1,4} = \frac{\lambda}{2} T_{total} \tag{19}$$

$$T_{2,3} = \frac{1-\lambda}{2} T_{total} \tag{20}$$

The total input power in the 4WID vehicle is

$$\begin{aligned} P &= 2 \times \left(\frac{\omega_1 T_1}{\eta_1(\omega_1, T_1)} + \frac{\omega_2 T_2}{\eta_2(\omega_2, T_2)}\right) \\ &= 2\left(\frac{\omega_{wh}\lambda T_{total}}{2\eta_0(\omega_{01}, T_{01})} + \frac{\omega_{wh}(1-\lambda)T_{total}}{2\eta_0(\omega_{02}, T_{02})}\right) \\ &= \omega_{wh} T_{total}\left(\frac{\lambda}{\eta_0(\frac{\omega_{wh}}{\alpha}, \frac{\lambda T_{total}}{2\beta})} + \frac{1-\lambda}{\eta_0(\frac{\omega_{wh}}{\alpha}, \frac{(1-\lambda)T_{total}}{2\beta})}\right) \\ &= P_0\eta_{gb}\left(\frac{\lambda\eta_0(\omega_0, T_0)}{\eta_0(\frac{\omega_0}{\alpha\zeta}, 2\lambda\alpha\zeta\eta_{gb}T_0)} + \frac{(1-\lambda)\eta_0(\omega_0, T_0)}{\eta_0(\frac{\omega_0}{\alpha\zeta}, 2(1-\lambda)\alpha\zeta\eta_{gb}T_0)}\right) \end{aligned}$$

Substitute the values of α, ζ and η_{gb}

$$P = P_0\left(\frac{\lambda\eta_0(\omega_0, T_0)}{\eta_0(1.5\omega_0, 1.3\lambda T_0)} + \frac{(1-\lambda)\eta_0(\omega_0, T_0)}{\eta_0(1.5\omega_0, 1.3(1-\lambda)T_0)}\right) \tag{21}$$

It is clear now that the total input power of the 4 in-wheel motors is dependent on the nonlinear distribution of the single traction motor efficiency map. The target of torque distribution is to find a λ, which can result in $P < P_0$, and equivalently,

$$\frac{\lambda\eta_0(\omega_0, T_0)}{\eta_0(1.5\omega_0, 1.3\lambda T_0)} + \frac{(1-\lambda)\eta_0(\omega_0, T_0)}{\eta_0(1.5\omega_0, 1.3(1-\lambda)T_0)} < 1 \tag{22}$$

A sufficient condition is to find the existence of $\lambda \in [0, 1]$, which satisfy both

$$\eta_0(1.5\omega_0, 1.3\lambda T_0) > \eta_0(\omega_0, T_0) \tag{23}$$

and

$$\eta_0(1.5\omega_0, 1.3(1-\lambda)T_0) > \eta_0(\omega_0, T_0) \tag{24}$$

Let $(\hat{\omega}_0, \hat{T}_0)$ denote an operation point in the work space of the single traction motor. If $(\hat{\omega}_0, \hat{T}_0)$ falls in the high efficiency region, obviously it will not be able to obtain a better performance. However, the high efficiency region is small, and we are still able to locate the operation points which satisfy (21). Beside the high efficiency region, operation points can also fall into two other regions discussed below.

1) Case 1: As shown in Fig. 3, the inner contours have higher efficiency. For $\hat{T}_0$, $\exists \hat{T}_{01}, \hat{T}_{02}$, $(\hat{T}_{01} < \hat{T}_{02})$ and $(1.5\hat{\omega}_0, \hat{T}_{0i})(i = 1, 2)$ are also in the same efficiency contour. Thus, if $2\hat{T}_{01} < 1.3\hat{T}_0 < 2\hat{T}_{02}$, we can find the optimal driving torque distribution (ODTD) strategy with better performance than the single traction motor configuration. In this case, $1.3\hat{T}_0$ can be divided into two torques, both of

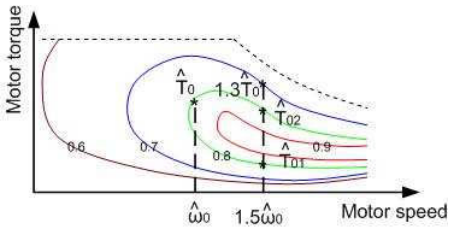

Fig. 3. Operation Point (Case 1)

which fall in the interval $[\hat{T}_{01}, \hat{T}_{02}]$ with higher efficiency. In summary, we express this condition as follows.

Condition 1:

For $(\hat{\omega}_0, \hat{T}_0)$, if there exist two operation points $(1.5\hat{\omega}_0, \hat{T}_{01})$ and $(1.5\hat{\omega}_0, \hat{T}_{02})$, which satisfy

$$\begin{cases} \eta_0(\hat{\omega}_0, \hat{T}_0) = \eta_0(1.5\hat{\omega}_0, \hat{T}_{0i}) \quad (i = 1, 2) \\ \hat{T}_{01} < 0.65\hat{T}_0 \\ \hat{T}_{02} > 0.65\hat{T}_0 \end{cases}$$

then we can find a λ to satisfy (21). Such operation point $(\hat{\omega}_0, \hat{T}_0)$ is in the sufficient condition region.

2) Case 2: If the operation points have low speed and low torque (Fig. 4), the efficiency contour has only one intersect $\hat{T}_{01}$ with the vertical $1.5\hat{\omega}_0$ line. In this case, the sufficient condition is $\hat{T}_{01} < 1.3\hat{T}_0 - \hat{T}_{01} < T_{max}(1.5\hat{\omega}_0)$, where $T_{max}(1.5\hat{\omega}_0))$ is the maximal continuous torque in at the speed $1.5\hat{\omega}_0$. More precisely, it can be derived as

Condition 2:

For point $(\hat{\omega}_0, \hat{T}_0)$, if there exist one and only one operation point $(1.5\hat{\omega}_0, \hat{T}_{01})$, which satisfy

$$\begin{cases} \eta_0(\hat{\omega}_0, \hat{T}_0) = \eta_0(1.5\hat{\omega}_0, \hat{T}_{01}) \\ 1.3\hat{T}_0 - T_{max}(1.5\hat{\omega}_0) < \hat{T}_{01} < 0.65\hat{T}_0 \end{cases}$$

then we can find a λ to satisfy (21).

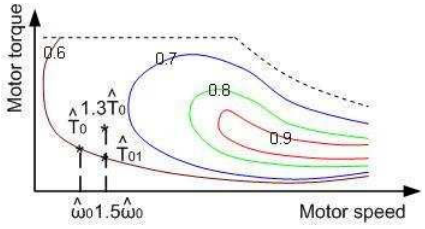

Fig. 4. Operation Point (Case 2)

The operation points complying the sufficient conditions of case 1 and 2 are evaluated computationally and denoted by red circles in the Fig. 5.

It can been observed that the the operation points complying the sufficient conditions covers approximately $\frac{1}{3}$ of the region with maximal peak torque, and it covers more than $\frac{1}{2}$ of the region with maximal continuous torque . They include in major the low-speed middle-torque states, which are the worst operational states for motors. The efficiency above the maximal continuous torque requires inaccurate external interpolation, so it is neglected.

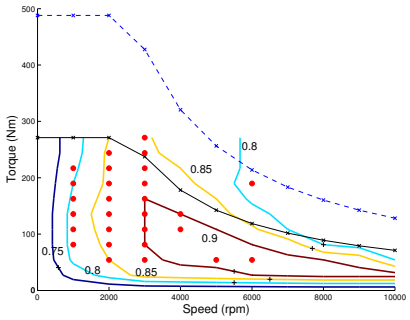

Fig. 5. Operation Region with Sufficient Condition for ODTD

One point to notice is that these conditions are sufficient but not necessary. In our simulation results, it is surprising that although a large quantity of operation points are not in the sufficient region, the energy saving results are still satisfactory. It attracts our interest to explore the necessary conditions in our further research.

IV. ENERGY MANAGEMENT STRATEGY

Because we are working with driving cycles, the time duration is fixed. Hence, the input energy optimization is equivalent to the input power optimization for each time interval.

Fig. 6 elaborates the system flow of the energy management strategy.

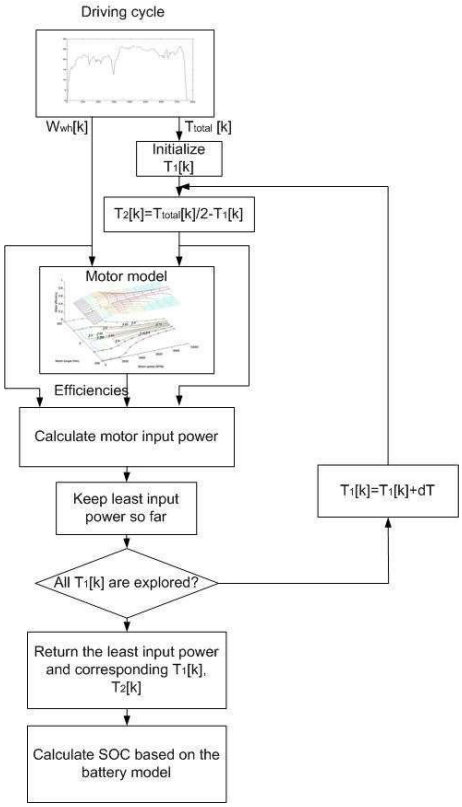

Fig. 6. System Flow

The total torque at time k, i.e. $T_{total}[k]$, and wheel

TABLE II
SIMULATION RESULT

Cycle	Item	Single Motor	ED	WPD	ODTD
HWYFET distance = 16.51km	ΔSOC	0.254	0.235	0.234	0.204
	$d_1\Delta$SOC	0	7.5%	7.8%	19.7%
	$d_2\Delta$SOC	-	0	0.0%	13.2%
UDDS distance= 11.99km	ΔSOC	0.179	0.142	0.142	0.130
	$d_1\Delta$SOC	0	20.7%	20.7%	27.4%
	$d_2\Delta$SOC	-	0	0	8.5%
JP10-15 distance= 4.16km	ΔSOC	0.059	0.051	0.051	0.044
	$d_1\Delta$SOC	0	13.6%	13.6%	25.4%
	$d_2\Delta$SOC	-	0	0%	13.7%

rotation speed at time k, i.e. $\omega_{wh}[k]$, are firstly calculated from the driving cycle based on the Section II. $k = 1, 2, ..., n$ is the sampled time sequence with step length $1s$. Then $(\omega_{wh}[k], T_1[k], T_2[k])$ are input to the motor efficiency map to evaluate $\eta_1[k]$ and $\eta_2[k]$, which together with $(\omega_{wh}[k], T_1[k], T_2[k])$, compose the necessary information to calculate the motor input power. Iteratively, all $T_1[k]$ in the torque domain are probed with step increment dT to find the minimal motor input power. dT is selected based on the coarseness of the motor efficiency map. In this paper, we adopt $dT = \frac{\tilde{T}_2 - \tilde{T}_1}{2}$. $\tilde{T}_2$ and $\tilde{T}_1$ are two adjacent torques in the torque axis of the motor efficiency map.

V. SIMULATION AND EXPERIMENT

Based on the Advisor in Matlab, we conducted simulation of torque distribution strategies for energy management in the 4WID vehicle, to compare with the Smartcar EV.

Aside of the optimal driving torque distribution (ODTD), we also carry out simulations with even distribution (ED), i.e. $T_i[k] = \frac{T_{total}}{4}$, $(i = 1, 2, 3, 4)$, and weighted proportional distribution (WPD) based on the static weight distribution, i.e. $T_{1,4}[k] = \frac{b}{a+b}\frac{T_{total}[k]}{2}$ and $T_{2,3}[k] = \frac{a}{a+b}\frac{T_{total}[k]}{2}$.

Table II illustrates the simulation results. 3 driving cycles, which are HWYFET (long distance), UDDS (mid distance), and JP10_15 (short distance) are tested. ΔSOC is the consumed total energy from the battery. $d_1\Delta$SOC is the percentage of energy saved among the five ΔSOCs. $d_2\Delta$SOC is the percentage of energy saved among ΔSOCs by the 4 torque distribution strategies. The results validates the effect the proposed ODTD strategy in 4WID vehicle energy management. The 4WID structure can save more than 13% energy compared with traditional EV; while ODTD strategy can save more than 19% and reaches maximally 27.4% in UDDS cycle. When the efficiency of gearbox (0.9 for operation points in general) in traditional EV is considered, the percentage of saved energy consumption will be approximated another 10% higher.

In Fig. 7, the operation points are shifted to the higher efficiency region in ODTD than the other 2 torque distribution strategies. Compared with Fig. 7(a), the efficiencies of the operation points in 4WID vehicle are generally higher.

Fig. 8 shows the difference in discharge powers between ED, WPD and ODTD, i.e. $\text{Power}_{\text{ED}} - \text{Power}_{\text{ODTD}}$, and $\text{Power}_{\text{WPD}} - \text{Power}_{\text{ODTD}}$ in the UDDS cycle. The non-negative difference validate the better performance of ODTD, and the integral of the difference in power is the input energy difference. Discharge power sequences of traditional EV and 4WID vehicle adopting ODTD strategy are illustrated in the lower subfigure of Fig. 8. The power consumption of traditional EV is mainly larger than that of the 4WID vehicle with ODTD. The figure is consistent with the test result in Table II.

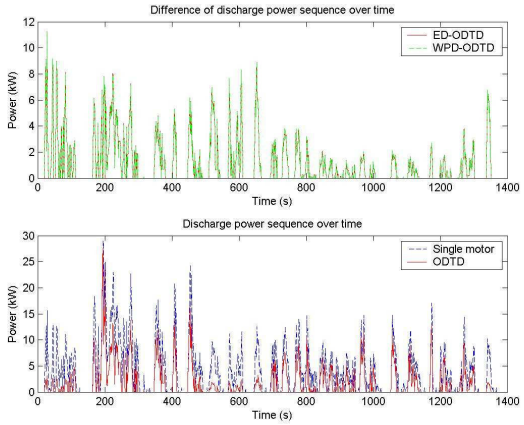

Fig. 8. Discharge Power Sequence

We have also developed a 4WID vehicle Omni-directional Kart-1 (OK-1, Fig. 9)[27], which adopts 4 in-wheel motors, so as to distribute torques for lower energy consumption. It is a experimental platform for future research. It can also have omni-directional motions, such as zero-radius turning and lateral parking, due to is 4 wheel independent steering configuration.

Fig. 9. 4WID Vehicle OK-1

VI. CONCLUSION

With the robotic 4WID configuration introduced into EV, the propelling task of the single traction motor in traditional EV can be shared cooperatively by 4 independent in-wheel motors. Hence, there will be extra DOF (in this paper, we explored 1 DOF, and actually there can be 3 DOF when torque distribution in left and right wheels are considered) which enables the total input power of the 4 motors to be optimized by means of increasing the motor efficiency.

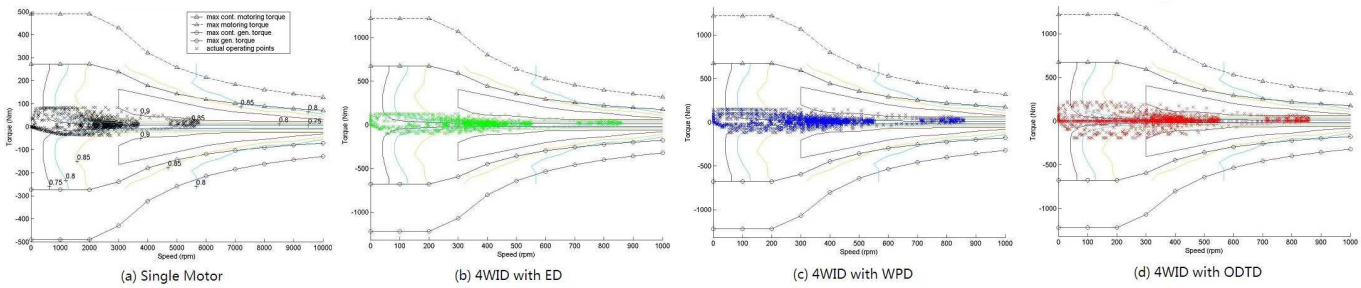

Fig. 7. Motor Operation Points (UDDS cycle)

For a meaningful comparison, the efficiency maps of the single traction motor and the in-wheel motor have the similar shape, only with two scaling factors in speed and torque to satisfy the different power requirement. Operation region with sufficient condition to discover the ODTD strategy is extracted. Simulation results validate the better performance of the 4WID configuration and the ODTD strategy. With the increasing number of commercial mobile robots, energy management will also attract more attention in the research field.

VII. ACKNOWLEDGMENTS

The authors gratefully acknowledge the valuable advise from Dr. Weimin Li on sharing of the HEV energy management knowledge.

This paper is partially supported by CAS project O945091001 (subproject "Key Technology Research in Energy Management and Drive Control for Harbor Water Quality Detector"), and Hong Kong ITF projects ITP/036/08AP, and GHP/006/09SZ.

REFERENCES

[1] J.W. Pavlat and R.W. Diller, "An energy management system to improve electric vehicle range and performance", *IEEE AES Systems Magazine*, June, 1993, pp. 3-5.

[2] Jinrui N., Fengchun S., and Qinglian R., "A study of energy management system of electric vehicles", *IEEE Vehicle Power and Propulsion Conference*, September, 2006, pp. 1-6.

[3] P.C.K. Luk and L.C. Rosario, "Power and energy management of a dual-energy source electric vehicle - policy implementation issues", *CES/IEEE 5th International Power Electronics and Motion Control Conference*, vol. 1, August, 2006, pp. 1-6.

[4] F. Badin, J. scordia, R. Trigui, E. Vinot, and B. Jeanneret, "Hybrid electric vehicles energy consumption decrease according to drive train architecture, energy management and vehicle use", *IET Hybrid Vehicle Conference*, December, 2006, pp. 213-224.

[5] D. Yin and Y. Hori, "A novel traction control of EV based on maximum effective torque estimation", *IEEE Vehicle Power and Propulsion Conference*, September 2008, pp. 1-6.

[6] K.J. Waldron and M.E. Abdallah, "An optimal traction control scheme for off-road operation of robotic vehicles", *IEEE/ASME Transactions on Mechatronics*, 2007, vol. 12, no. 2, pp. 126-133.

[7] J. Zhang, D. Chen, and C. Yin, "Adaptive fuzzy controller for hybrid traction control system based on automatic road identification", *Proceeding of the 2006 IEEE International Conference on Automation Science and Engineering*, 2006, pp 524-529.

[8] S. Pannacchio and D. Rizzo, "Intelligent traction control for wheel space vehicle", *10th IEEE Conference on Emerging Technologies and Factory Automation*, September, 2005, pp. 235-240.

[9] J. Burg and P. Blazevic, "Anti-lock braking and traction control concept for all-terrain robotic vehicles", *Proceedings of the 1997 IEEE International Conference on Robotics and Automation*, 1997, pp. 1400-1405.

[10] S. Sakai, H. Sado, and Y. Hori, "Motion control of an electric vehicle with four independently driven in-wheel motors", *IEEE Transactions on Mechatronics*, 1999, vol. 4, no. 1, pp. 9-16.

[11] K. Fujii and H. Fujimoto, "Traction control based on slip ratio estimation without detecting vehicle speed for electric vehicle", *2007 Power Conversion Conference - Nagoya*, 2007, pp. 688-693.

[12] Q. Chen and Y. Zhan, *Electric Vehicle – the Green Transportation Tool for the 21st Century (in Chinese)*, Tsinghua University Press and Jinan University Press, 2000.

[13] J. Malinowski, "Specifying energy efficienty motors in industry standards", *Energy Efficiency in Motor Driven Systems*, Springer, 2003, pp.373-377.

[14] H. Shen, etc., *Motor Engineering Manual (in Chinese)*, Mechanical Industry Press, 1982.

[15] Z. Wang, W. Li, and Y. Xu, "A novel power control strategy of series hybrid electric vehicle", *Proceedings of the 2007 IEEE/RSJ International Conference on Intelligent Robots and Systems*, October-Novermber, 2007, pp.96-102.

[16] J.T.B.A. Kessels, M.W.T. Koot,;P.P.J. van den Bosch, and D.B. Kok, "Online energy management for hybrid electric vehicles", *IEEE Transactions on Vehicular Technology*, vol. 57, iss. 6, November, 2008, pp. 3428-3440

[17] W. Li, G. Xu, Z. Wang, and Y. Xu, "Dynamic energy management for hybrid electric vehicle based on approximate dynamic programming", *Proceedings of the 7th world Congress on Intelligent Control and Automation*, June, 2008, pp.7864-7869.

[18] M.H. Hajimiri and F.R. Salmasi, "A fuzzy energy management strategy for series hybrid electric vehicle with predictive control and durability extension of the battery", *2006 IEEE Conference on Electric and Hybrid Vehicles*, December, 2006, pp. 1-5.

[19] http://www.toyota.com/prius-hybrid/

[20] http://automobiles.honda.com/civic-hybrid/

[21] http://www.treehugger.com/files/2008/12/byd-f3dm-electric-plug-in-hybrid-china.php

[22] http://www.nissan-global.com/EN/PIVO2/

[23] D. Ratner and P. M^c'Kerrow, "Using LabVIEW to prototype an industrial-quality real-time solution for the Titan outdoor 4WD mobile robot controller", *Proceedings of 2000 IEEE/RSJ International Conference on Intelligent Robots and Systems*, 2000 vol. 2 October-Novermber, 2000, pps. 1428-1433.

[24] M. Wada, "Studies on 4WD mobile robots dlimbing up a step", *Proceedings of the 2006 IEEE International Conference on Robotics and Biomimetics*, December, 2006, pp. 1529-1534.

[25] F.J. Wang and B. Zhang, "Path tracking control for a four wheel differentially steered vision robot", *2008 International Conference on Electrical Machines and Systems*, October, 2008, pp. 1608-1611.

[26] S. Amagai, T. Tsuji, J. Samuel, and H. Osumi, "Control of omni-directional mobile platform with four driving wheels using torque redundancy", *2008 IEEE/RSJ International Conference on Intelligent Robots and Systems*, September, 2008, pp. 1996-2002.

[27] H. Qian, T.L. Lam, W. Li, C. Xia, and Y. Xu, "System and design of an omni-directional vehicle", *Proceedings of the 2008 IEEE International Conference on Robotics and Biomimetics*, February, 2009, pp. 389-394.